Use of SCADA Data for Failure Detection in Wind Turbines

K. Kim, G. Parthasarathy, O. Uluyol, and W. Foslien
Honeywell

S. Sheng and P. Fleming
National Renewable Energy Laboratory

NOTICE

Available electronically at http://www.osti.gov/bridge

Available for a processing fee to U.S. Department of Energy
and its contractors, in paper, from:

> U.S. Department of Energy
> Office of Scientific and Technical Information
>
> P.O. Box 62
> Oak Ridge, TN 37831-0062
> phone: 865.576.8401
> fax: 865.576.5728
> email: mailto:reports@adonis.osti.gov

Available for sale to the public, in paper, from:

> U.S. Department of Commerce
> National Technical Information Service
> 5285 Port Royal Road
> Springfield, VA 22161
> phone: 800.553.6847
> fax: 703.605.6900
> email: orders@ntis.fedworld.gov
> online ordering: http://www.ntis.gov/help/ordermethods.aspx

Cover Photos: (left to right) PIX 16416, PIX 17423, PIX 16560, PIX 17613, PIX 17436, PIX 17721

Printed on paper containing at least 50% wastepaper, including 10% post consumer waste.

USE OF SCADA DATA FOR FAILURE DETECTION IN WIND TURBINES

Kyusung Kim
Honeywell
Golden Valley, MN, USA

Girija Parthasarathy
Honeywell
Golden Valley, MN, USA

Onder Uluyol
Honeywell
Golden Valley, MN, USA

Wendy Foslien
Honeywell
Golden Valley, MN, USA

Shuangwen Sheng
NREL
Golden, CO, USA

Paul Fleming
NREL
Golden, CO, USA

ABSTRACT

High operations and maintenance costs for wind turbines reduce their overall cost effectiveness. One of the biggest drivers of maintenance cost is unscheduled maintenance due to unexpected failures. Continuous monitoring of wind turbine health using automated failure detection algorithms can improve turbine reliability and reduce maintenance costs by detecting failures before they reach a catastrophic stage and by eliminating unnecessary scheduled maintenance. A SCADA-data based condition monitoring system uses data already collected at the wind turbine controller. It is a cost-effective way to monitor wind turbines for early warning of failures and performance issues. In this paper, we describe our exploration of existing wind turbine SCADA data for development of fault detection and diagnostic techniques for wind turbines. We used a number of measurements to develop anomaly detection algorithms and investigated classification techniques using clustering algorithms and principal components analysis for capturing fault signatures. Anomalous signatures due to a reported gearbox failure are identified from a set of original measurements including rotor speeds and produced power.

INTRODUCTION

Among the challenges, noted in the DOE-issued report '20% Wind Energy by 2030' [1], are improvement of wind turbine performance and reduction in operating and maintenance costs. After the capital costs of commissioning wind turbine generators, the biggest costs are operations, maintenance, and insurance [1-3]. Reducing maintenance and operating costs can considerably reduce the payback period and provide the impetus for investment and widespread acceptance of this clean energy source.

Maintenance costs can be reduced through continuous, automated monitoring of wind turbines. Wind turbines often operate in severe, remote environments and require frequent scheduled maintenance. Unscheduled maintenance due to unexpected failures can be costly, not only for maintenance support but also for lost production time. In addition, as wind turbines age, parts fail, and power production performance degrades, maintenance costs increase as a percentage of production. Monitoring and data analysis enables condition-based rather than time-interval-based maintenance and performance tune-ups. Experience from other industries shows that condition monitoring detects failures before they reach a catastrophic or secondary-damage stage, extends asset life, keeps assets working at initial capacity factors, enables better maintenance planning and logistics, and can reduce routine maintenance.

Traditionally, condition monitoring systems for wind turbines have focused on the detection of failures in the main bearing, generator, and gearbox, some of the highest cost components on a wind turbine [4–6]. Two widely-used methods are vibration analysis and oil monitoring [4, 5, 7, 8]. These are standalone systems that require installation of sensors and hardware. A supervisory control and data acquisition (SCADA) -data based condition monitoring system uses data already being collected at the wind turbine controller and is a cost-effective way to monitor for early warning of failures and performance issues.

In this paper, we describe our exploration of existing wind turbine SCADA data for development of fault detection and diagnostic techniques. Our ultimate goal is to be able to use SCADA-recorded data to provide advance warning of failures or performance issues. For the work described here, we used data from the Controls Advanced Research Turbine 2 (CART2) at the National Wind Technology Center (NWTC) at the National Renewable Energy Laboratory (NREL). A number of measurements from the turbine are used to develop anomaly detection algorithms. Classification techniques such as clustering and principal components analysis were investigated

for capturing fault signatures. The developed algorithms were tested with data from a failed gearbox incident. The next two sections give a survey of failure modes and the current state of condition monitoring in wind turbines. We then describe the wind turbine and data used for this work, followed by a description of the detection algorithm approaches, results, discussion, and concluding remarks.

FAILURE MODES IN WIND TURBINES

A condition-based monitoring (CBM) system must be designed to provide maximum benefit for its cost. Since not every failure can be detected ahead of time nor prevented, it makes sense to target the failures that are most costly to repair. After reviewing publications [9–15] that provide survey data on wind turbine field failures, we summarized the failure rates of wind turbine subsystems. Our emphasis was on learning which subsystems were most costly to repair, not just the frequency of failures. While the cost of repair or replacement information is not available in the surveys, we could use downtime as an indirect indicator of cost and effort to repair. Downtime provides an additional measure of lost revenue due to failure. We determined the ranks of the subsystems by failure rate and downtime per turbine per year, by summarizing all surveys reviewed above. Fig. 1 is a graphical representation of the average failure rate and downtime. Note that in the surveys and Fig. 1, gearbox failures are separated from other drivetrain component failures.
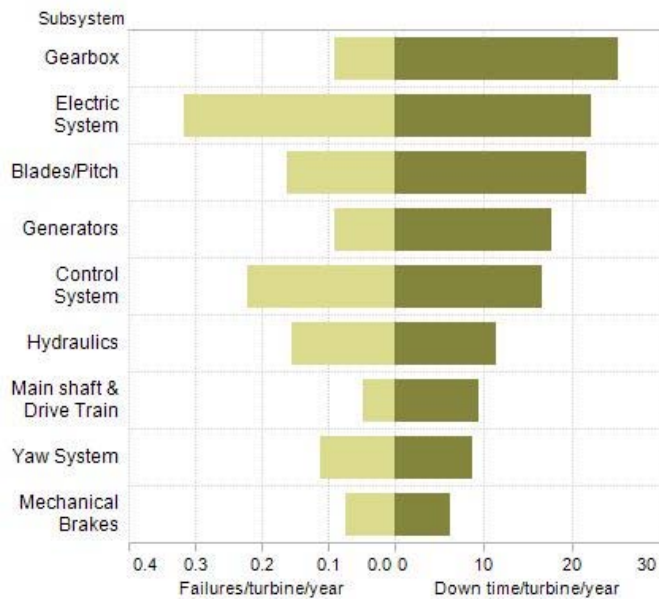
FIG. 1. LITERATURE REVIEW SUMMARY OF FAILURE RATE AND DOWNTIME/TURBINE/YEAR

Some surveys present downtime as downtime/ turbine/year, others present it as downtime/failure. We present the information as downtime/turbine/year, because it captures frequency of failure as well as downtime per failure. We find that although large subsystems such as gearboxes fail infrequently, these failures result in the most downtime per turbine, per year. Anecdotal comments from wind farm owners and operators suggest that gearbox failures dominate the cause for concern. However, as seen in Fig. 1, other failures are not far behind. A monitoring system that provides detection coverage for multiple top failure modes will be valuable in a maintenance system. With this objective, we explore the use of SCADA data for fault detection and diagnostics.

CONDITION MONITORING IN WIND TURBINES

Most of the literature about condition monitoring of wind turbines focuses on gearboxes and other drivetrain components [16–18]. This is consistent with the conclusions from the survey of wind turbine failure modes, where the gearbox failures contribute to the most costly repairs. Vibration-based approaches and oil monitoring techniques are the most mature, having been applied to large rotating machinery in other domains. Some are being applied to wind turbines at a research or pilot scale [5]. One comprehensive study is being conducted at NREL, using both dynamometer and field turbines as testing platforms [5]. Other techniques that are being developed in a lab or pilot setting are acoustic emission sensors, wavelet analysis for vibration signatures, and electrical current and power signatures [5, 19]. In some cases, SCADA data, mainly temperature (bearing or generator winding), have been used along with vibration data for fault detection [6, 19]. Operating data also is used to normalize the vibration or temperature data [6, 20]. Zaher [2] presented a method to use SCADA data for anomaly detection based on neural network models of normal operating modes. Use of SCADA data for fault diagnostics and prognostics algorithms in wind turbines is not as mature as in other industries, such as process and aerospace, where the use of condition-based maintenance is more widespread.

WIND TURBINE DIAGNOSTICS WITH SCADA DATA

SCADA or operating data of equipment has been used in other industries for accurate and timely detection, diagnostics and prognostics of failures and performance problems [22–27]. For example, in turbine engine diagnostics, failures such as turbine degradation, compressor bleed band failure, fuel supply system faults, combustion liner burn-through, and in-range sensor faults can be automatically detected with appropriate diagnostic algorithms. SCADA data provides a rich source of continuous time observations, which can be exploited for overall turbine performance monitoring. With appropriate algorithms, performance monitoring can be matured into individual component fault isolation schemes.

Performance is described in the context of the underlying process physics of the equipment—in this case, the wind turbine. The wind turbine converts wind kinetic energy into useful electrical energy. As turbine components deteriorate, the efficiency with which wind energy is converted to electrical energy decreases and the performance of the turbine decreases. Performance degradation can indicate problems such as blade aerodynamic degradation due to leading and trailing edge losses, dirt or ice buildup on blades, loss due to drivetrain misalignment, friction caused by bearing or gear faults, generator winding faults, or even pitch control system

degradation. The functional elements of performance monitoring are shown in Fig. 2. A performance parameter is first computed based on sensor measurements; this parameter could be raw sensor values, sensor values corrected for environmental conditions, residuals with respect to a wind turbine model, component efficiency or aerodynamic parameters. Anomaly detection uses one or more such parameters to test whether the wind turbine is behaving within normal bounds. If the root cause of the anomaly is further classified as a particular component failure, this provides diagnosis. Additional elements involve predictive trending and prognostics, wherein parameters or fault indicators are trended, and time to failure is projected.
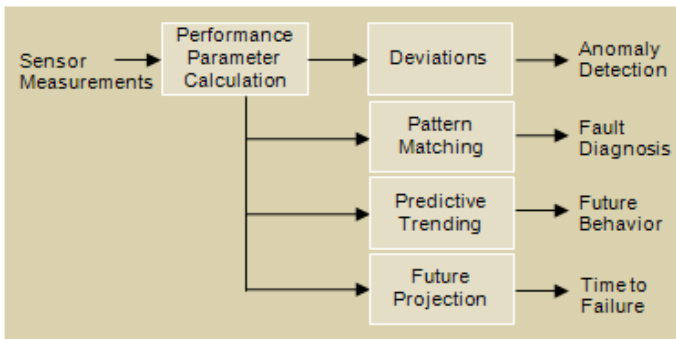

FIG. 2. SCADA DATA BASED MONITORING

Anomaly detection can be performed with a series of techniques that range from simple threshold checks to complex statistical analyses. Here, we focus on anomaly and fault detection methods for analyzing sensor data from indivi-dual wind turbines. Sensor data used in algorithm development and the approaches are described in the next sections.

DESCRIPTION OF CART TURBINE AND DATA

The Controls Advanced Research Turbine 2 (CART2) is a modified Westinghouse® WWG-0600 machine rated at 600 kW. It is located at the NWTC at NREL in Colorado and was installed to test new control schemes for power and load regulation. In its original configuration, the WWG-0600 uses a synchronous generator, fluid coupling, and hydraulic collective pitch actuation. To enable advanced control research for variable speed wind turbines, the CART2 has been retrofitted with an induction generator, rigid coupling, and individual electromechanical pitch actuators. The rotor runs upwind of the tower and consists of two blades and a teetering hub [27]. As a research turbine, it is outfitted with many more sensors (see Fig 3) than would normally be installed on commercial turbines, including pressure transducers, torque transducers, strain gauges, thermometers, position encoders, accelerometers, anemometers, wind vanes, and power, current, and voltage meters. The output of each of these sensors is recorded at the control rate of 100 Hz. Eighty-eight measurements are stored in ten-minute blocks including: pitch angles, shaft torque, oil temperature and pressure, yaw positions, wind speeds and

directions, ambient temperature, 12 vibrations, tower loads, generator power/current/voltage, and other control signals.
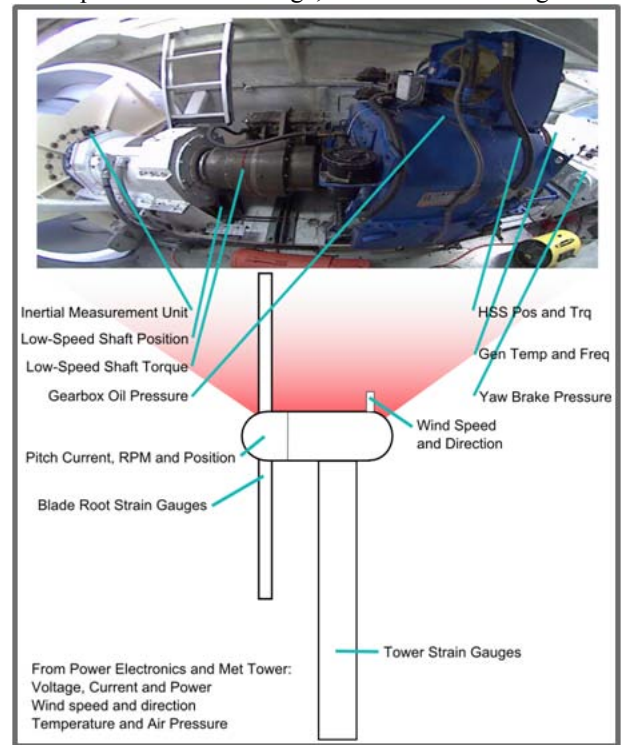

FIG. 3. CART2 SENSOR LOCATIONS [33]

NON-LINEAR PCA

The sensor data contain information about the state of the system being observed as well as redundant information and noise. Principal component analysis (PCA) is often used to extract useful and non-redundant information from the sensor data. PCA is a linear data analysis method that can produce orthogonal principal directions along which the data exhibit the largest variances. Because it is limited to capturing linear relationships, an extension to the nonlinear domain may be considered. An auto-associative neural network (AANN) approach provides one of the ways of implementing nonlinear PCA.

An AANN processes the input data through five sequential layers, one input layer, three hidden layers composed of a mapping layer, a bottleneck layer, and a de-mapping layer, and one output layer, as shown in Fig. 4, to produce an output that is identical to the input at the final layer [21]. This type of network learns an approximation of the identity mapping between the inputs and the outputs. The network contains a bottleneck at its third layer that compresses the information, allowing the network to learn a correlation model for the input data.
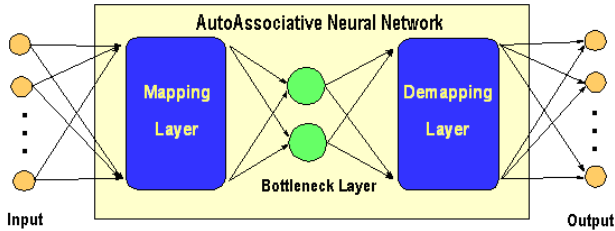
FIG. 4. AANN WITH THREE HIDDEN LAYERS, PLUS INPUT AND OUTPUT LAYERS

The network develops an internal representation of the data. As the data is mapped from one layer to another, linear or nonlinear transfer functions are used. The internal (compressed) representation obtained at the bottleneck layer through a nonlinear transfer function corresponds to nonlinear principal components of the input data [29]. The network is trained with data from normal operation. When presented with a set of new inputs, it can then produce a small set of principal components that can be trended or otherwise processed to detect changes in the underlying nonlinear dynamics of the system.

To map the changes seen in the principal components into anomaly detection and fault isolation indicators, the Q statistic and Hotelling T^2 statistics are computed. The Q statistic is a measure of the amount of variation not captured by the linear or nonlinear PCA model while the T^2 statistic is a measure of the variation in the model.

CLUSTERING TECHNIQUES— SELF-ORGANIZING FEATURE MAPS

Clustering algorithms are methods for dividing a set of *n* observations into *g* groups, called *clusters*, so that members of the same group are more alike than members of different groups. When class labels of observations are available, supervised learning techniques are used to learn the observations; otherwise, unsupervised learning is appropriate. In unsupervised learning, no target outputs are available, so the free parameters, such as weights and biases in a neural network, are modified only in response to network inputs. They categorize the input patterns into a number of classes.

A self-organizing feature map (SOFM) is a type of unsupervised clustering algorithm that forms neurons located on a regular grid, usually in one or two dimensions [30]. The cluster representatives that are the neurons in the layer of a SOFM are initially assigned at random, in some suitable distribution according to a topology function, that dictates the structure of the map. SOFM can detect regularities and correlations in its input and adapt its future responses to that input by learning to classify input vectors. Based on the competitive learning process, the neurons become selectively tuned to input patterns so that neurons physically near each other in the neuron layer respond to similar input vectors. Since the health condition (normality or failure) for each data point is not available in the field, SOFMs are particularly suited to find patterns in the data, without target class labels. Fig. 5 illustrates

the training and operating steps in using the SOFM technique [31].
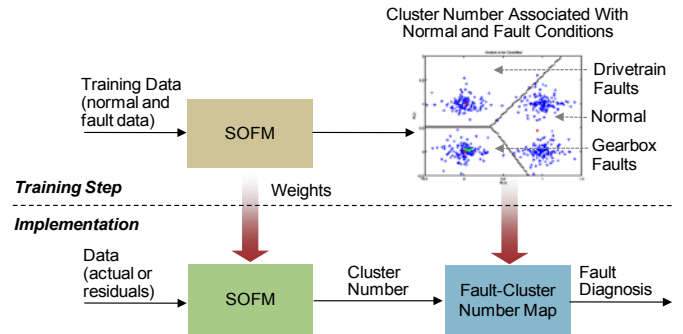
FIG. 5. FAULT DIAGNOSIS USING SOFM

DEVELOPMENT APPROACH

In our work, wind turbine data is segmented according to the wind turbine operating regime (Fig. 6). Different control schemes govern different regimes [32]. In order to differentiate real fault signatures from similar operational signatures, data is partitioned and signatures are compared from the same operating regimes. Our focus is on data from operating Region 2 in Fig. 6.

Data preprocessing also includes modification of the sampling rate. The original CART2 data was collected at the sampling rate of 100 Hz, as CART2 is used mainly to test control schemes. Although such high frequency data contains richer information enabling superior fault detection, we down-sampled the original data set to 1 Hz. Down-sampling may be used because the fault signatures are still observable from the lower sampled data. Also, a main objective of this work is to use SCADA data for CBM purposes, and the sampling frequency of SCADA data is much slower, typically one sample per minute.
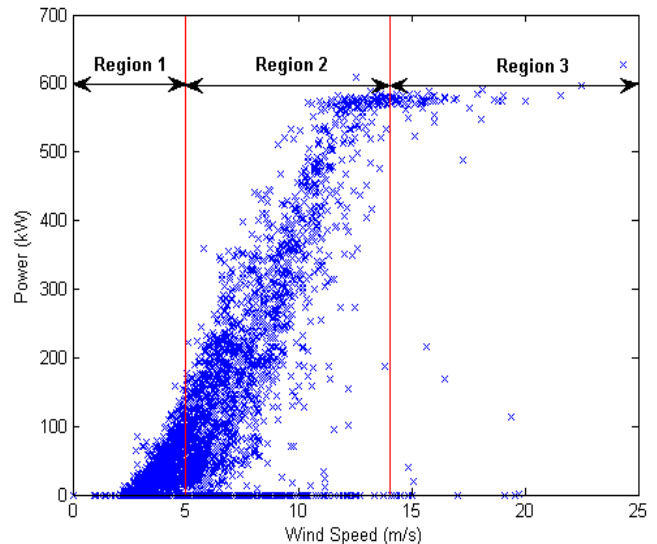

FIG. 6. WIND TURBINE OPERATION REGION

A gearbox-related failure was reported for CART2. We obtained the data measured around the time of failure along

with data sets collected before and after the failure. The data sets were analyzed to explore patterns in the data. Trends in individual measurements, different combinations of individual measurements, and their relationships to other measurements were analyzed. Fig. 7 and Fig. 8 show results of some of this analysis. In both figures, the circles represent faulty data and the Xes represents normal, baseline data. Fig. 7 (Fault Indications A) shows the variations in the ratio of high-speed shaft (HSS) torque to HSS speed versus the power level. This figure shows a clear distinction between the fault and the baseline, especially at relatively lower power levels (< 400 kW).
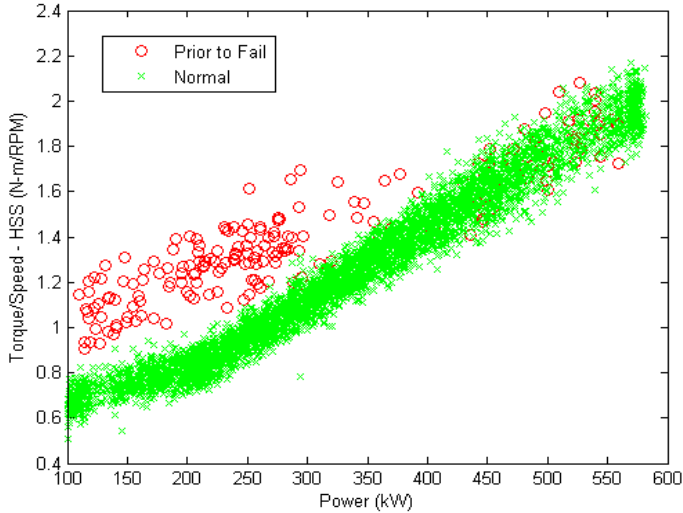
FIG. 7. OBSERVED FAULT INDICATIONS A
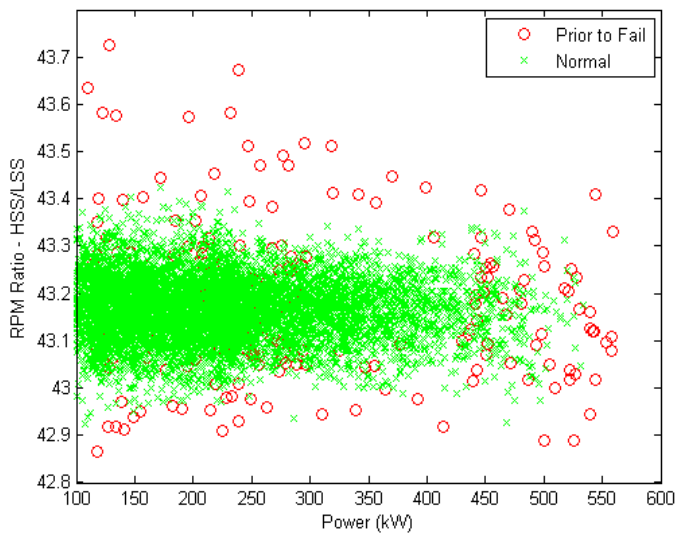
FIG. 8. OBSERVED FAULT INDICATIONS B

The variation of the ratio of HSS speed to LSS speed versus power level is shown in Fig. 8 (Fault Indications B). In this case, the distinction between the fault and the baseline can still be observed, although the indication is not as strong as in Fig. 8—the variation of the speed ratio from fault data is much larger across every power level and overlaps with the variation from the baseline data.

Based on these observations, fault detection and isolation algorithms are developed using PCA and SOFM. The alarms are generated based on three indicators: two indicators from PCA based on Q-stat and T^2, and one indicator from the SOFM based on the clusters. During the training stage, two training sets were prepared. One set was composed of power, HSS torque, and HSS speed, and the other set was composed of power, HSS torque, HSS speed, and LSS speed. The first set captures the fault indication observed from Fig. 7, and the second set captures the fault indications observed from Fig. 7 and Fig. 8.

The data set used to train the AANN was prepared to ensure that it represented the widest possible operation range within the Region 2, defined earlier. In fact, the training/testing data set consists of data collected from operations over a period of two years. The training/test data set for the AANN is composed of baseline data only. AANN training is done with varying numbers of nodes at the bottleneck, mapping, and de-mapping layers. The number of nodes at the bottleneck layer is always smaller than the number of nodes at the mapping and input layers. Having trained the model based on the two sets described above, we found that the AANN trained with the first set performed better, and resulted in fewer false alarms with more successful detection. We believe this occurs because the wider spread of the speed ratio, from the fault data shown in Fig. 7, makes the fault and normal data less separable. The better performance of the model trained with the first data set also is observed when training the SOFM.

The only difference between the training set used for SOFM and the training set used for AANN is that the SOFM training set must include the fault data. Thus, the SOFM training data set is an augmentation of the AANN training set, with the addition of the fault data. The SOFM training involves varying the number of nodes.

RESULTS AND DISCUSSION

Fig. 9 shows the Q-stat and T^2 values obtained from the AANN using the training data set, which represents the baseline. The horizontal line represents the threshold indicating anomalies when the Q-stat or T^2 of a sample rises above the limit. Based on the variability seen in the training set, the thresholds are set at the six sigma level for Q-stat and the three sigma level for T^2, respectively.
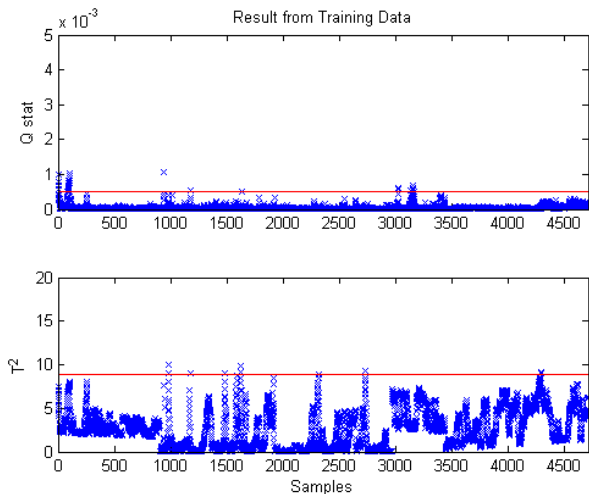
FIG. 9. NON-LINEAR PCA OUTPUT FROM TRAINING SET

The result from another test data set that was not part of the training data is shown in Fig. 10. This data set covers all seasons and includes no reported incidents.
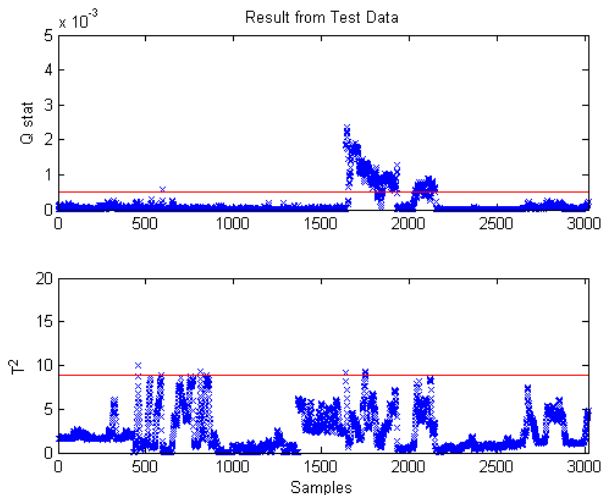

FIG. 10. NON-LINEAR PCA OUTPUT FROM TEST DATA (NOT USED IN TRAINING PROCESS)

A portion of the data samples cross the threshold of Q-stat. This portion corresponds to the unknown anomalies. Even though no confirmed incidents occurred in that time frame, this indicates samples that do not fit the non-linear PCA model developed from the training data set. With the current threshold set at the six sigma level from the training set, there will be triggers for any other anomalies that are not covered by the training set. A specific event we want to detect is a gearbox failure incident that occurred in CART2. The Q-stat values from the samples (Fig. 11) obtained during the incident show very large values compared to those from the training or other test data set (Fig. 9 and Fig. 10). These large values enable us to set the threshold at a much higher level so that the alarm is triggered only for the target failure and less sensitive to other unknown anomalies.

The result from the data collected on the day when the gearbox failure occurred is shown in Fig. 11. Both Q-stat and

T^2 display large values. The samples of Q-stat or T^2 values exceeding the threshold indicate that they are not representative of the data used to develop the AANN, which corresponds to the baseline condition.
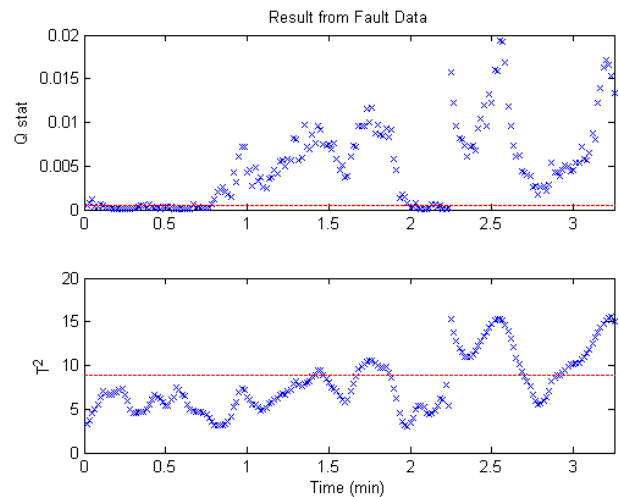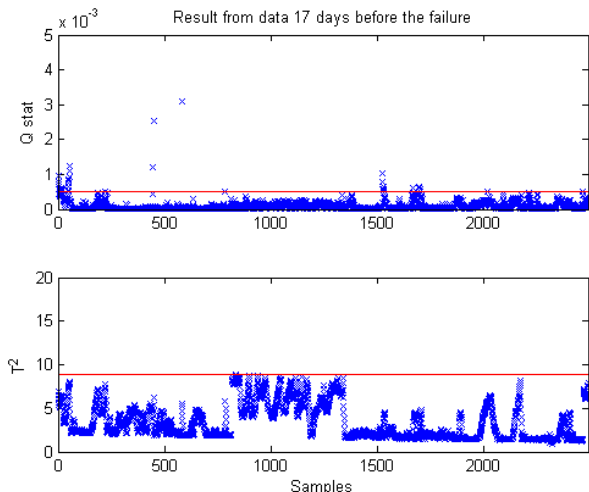

FIG. 11. NON-LINEAR PCA OUTPUT FROM FAILURE CASE

Results from the data collected before the failure are shown in Fig. 12 and Fig. 13.
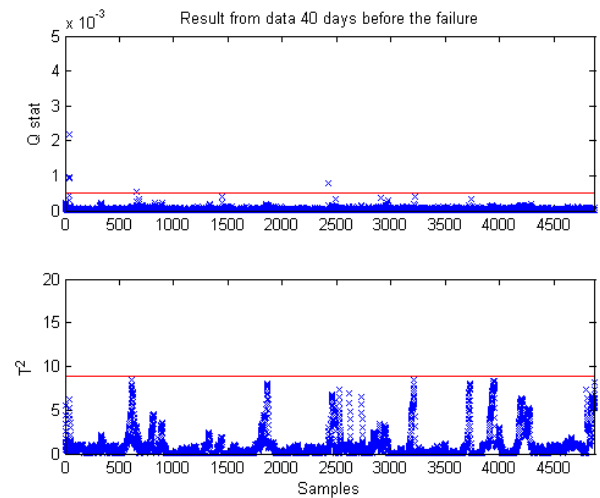
**FIG. 12. NON-LINEAR PCA OUTPUT 40 DAYS BEFORE THE FAILURE**

6

FIG. 13. NON-LINEAR PCA OUTPUT 17 DAYS BEFORE THE FAILURE

The data obtained 40 days before the failure is shown in Fig. 12, and Fig. 13 is the data obtained 17 days before the failure. A few samples cross the thresholds but the indication is not strong or persistent, as shown in Fig. 11. These days were chosen because they were closest to the failure and had data that was available to us. The log book indicates that the failure was suspected 14 days before it occurred. Unfortunately, data for the days leading up to the failure were not available. Additional analysis on the consistency of the alarms and lead time for early failure detection can be done only when additional data leading up to a failure becomes available. Tuning thresholds early to maximize accurate detection and to minimize false positives also can be done with additional data.

The result from the SOFM training is shown in Fig. 14.
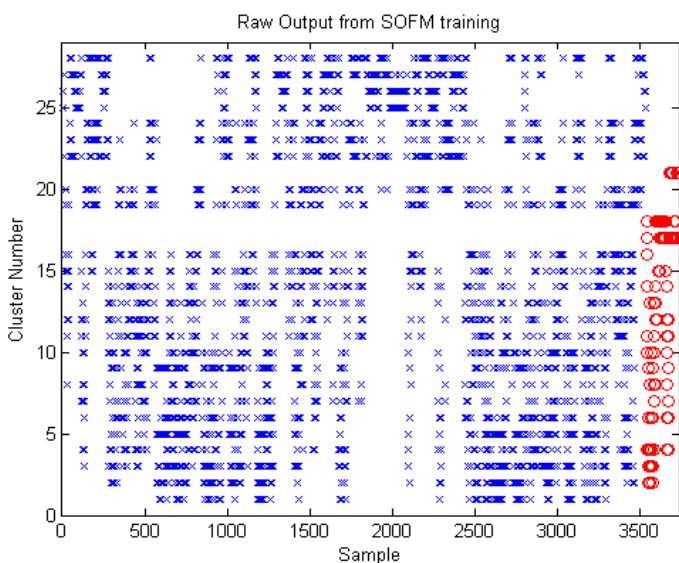
FIG. 14. SOFM OUTPUT FROM TRAINING SET

As mentioned above, the SOFM training set includes not only sufficient baseline data but also the fault data. The baseline data are shown as xes and include the data from the samples to around 3500. The data marked with os and corresponding to the

samples after 3500 are the fault data. The y-axis represents the cluster number. A clustering system of 28 clusters is obtained after the training; the y-axis shows the cluster number from 1 to 28. Notice that no baseline samples correspond to clusters 17, 18, and 21 and only the samples from the fault data correspond to these clusters. This indicates that clusters 17, 18, and 21 are formed based on the fault data only; thus, they represent the fault condition. Some clusters are not observed in the baseline data samples because baseline data samples are obtained from various operating conditions. The remaining clusters correspond to the baseline data and represent the normal condition. Depending on the separation between the fault baseline data, the fault or baseline conditions can be represented by multiple clusters.

Based on this information, the cluster numbers are mapped into the normal and fault conditions. The faulty data set as shown in Fig. 15.
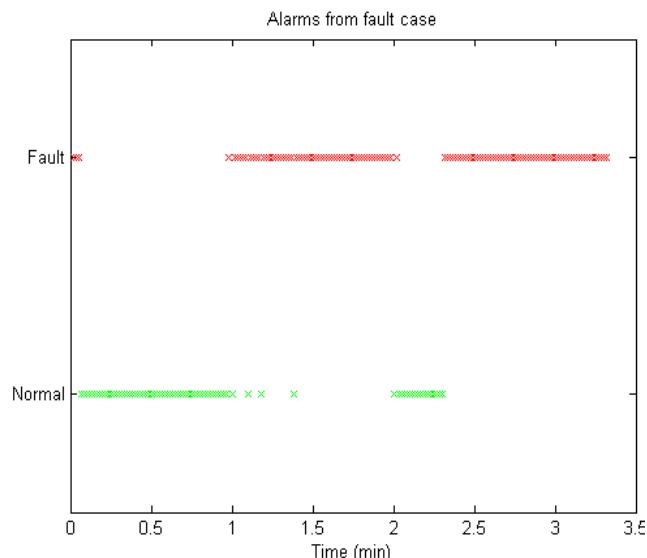

FIG. 15. SOFM OUTPUT FROM FAULT CASE AFTER MAPPING THE CLUSTERS INTO CONDITIONS

The samples shown in Fig. 15 correspond to the last 3.5 minutes of the data marked in Fig. 14. This illustrates how an alarm based on this diagnostic technique might function in practice. Although SOFM can isolate faults, it is trained in only one failure mode, as that is the only failure history available. If other failure modes are observable from the same set of parameters, a SOFM can demonstrate its isolation capability by forming other clusters that correspond to new failure modes. In that case, two different alarms indicating two different failure modes will be generated. Fig. 16 shows the result from the data closest to the failure day among the data available. As noted earlier, no fault is indicated yet. The comparison of alarms triggered by three different indicators is shown in Fig. 17—two indicators from AANN based on Q-stat and T^2 and one indicator from SOFM based on the clusters. The alarms are consistent, i.e. when T^2 triggers the other two also trigger. Compared to T^2, earlier detection is possible from Q-stat and SOFM. The three indicators seem to complement each other

well. For the brief periods, when one of the indicators does not trigger, the others provide a fault detection signal consistent with the indications in the neighboring time points. This finding shows that the three indicators presented in this research form a good set to include in a fusion scheme for increased robustness across indicators and along the time axis during a failure progression.
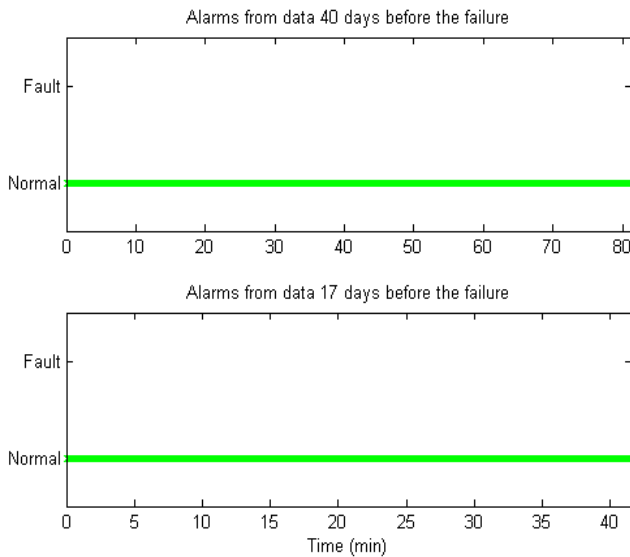
FIG. 16. SOFM OUTPUT BEFORE THE FAILURE AFTER MAPPING THE CLUSTERS INTO CONDITIONS
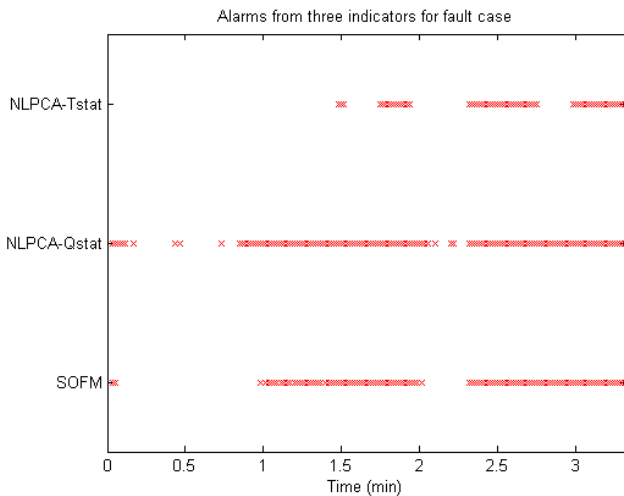
FIG. 17 COMPARISON OF ALARMS FROM THREE INDICATORS

SUMMARY

In this work, we presented an approach for fault detection using available SCADA-data from wind turbines. Systematic analysis of data indicated clear distinctions between fault and no-fault conditions in relationships among several parameters. These distinctions in relationships were exploited in the development of automated fault diagnostics algorithms. Two approaches, PCA and SOFM, were used in the algorithms. Both approaches are successful in producing persistent indicators that are well-distinguished from those generated based on no-fault data. Future work in maturing the approaches involves testing and tuning the algorithms, using additional data from the same and other wind turbines, and developing a fusion scheme for increased robustness and early fault detection.

REFERENCES

[1] '20% Wind Energy by 2030: Increasing Wind Energy's Contribution to U.S. Electricity Supply', http://www1.eere.energy.gov/windandhydro/wind_2030.html

[2] Zaher, A,, McArthur, S.D.J., Infield, D.G., Patel, Y. "Online Wind Turbine Fault Detection Through Automated SCADA Data Analysis," Wind Energy, 2009, Published online in Wiley Interscience (www.interscience.wiley.com) DOI: 10.1002/we.319.

[3] Musial, W. Butterfield, S., McNiff, B. "Improving Wind Turbine Gearbox Reliability," 2007 European Wind Energy Conference. http://www.nrel.gov/wind/pdfs/41548.pdf

[4] Crabtree, C.J. 'Survey of Commercially Available Condition Monitoring Systems for Wind Turbines', SuperGen Wind, November 2010.

[5] Sheng, S., Oyague, F. and Butterfield, S, "Investigation of Various Wind Turbine Condition Monitoring Techniques", 7th International Workshop on Structural Health Monitoring, Stanford University, Stanford, Sept 2009.

[6] Wiggelinkhuizen, E.; Verbruggen, T.; Braam, H.; Rademakers, L.; Xiang, J. and Watson, S., "Assessment of condition monitoring techniques for offshore wind farms," J. Sol. Energy Eng. 130, 031004, 2008.

[7] *Condition Monitoring of Wind Turbines: Technology Overview, Seeded-Fault Testing, and Cost-Benefit Analysis*. EPRI, Palo Alto, CA: 2006. 1010419.

[8] Amirat, Y.; Benbouzid, M.E.H.; Bensaker, B.; Wamkeue, R.; "Condition Monitoring and Diagnosis in Wind Energy Conversion Systems: A Review," *Electric Machines & Drives Conference, 2007. IEMDC '07. IEEE International* , vol.2, no., pp.1434-1439, 3-5 May 2007

[9] Ribrant, J. and Bertling, L. M. "Survey of Failures in Wind Power Systems with Focus on Swedish Wind Power Plants during 1997-2005," IEEE Tran. on Energy Conversion, Vol. 22, No. 1, March 2007.

[10] Annual Report on Performance of Wind Power Plants, VTT, http://www.vtt.fi/publications/

[11] Annual Report from ISET, http://www.windmonitor.de/

[12] Tavner, P. Spinato, J. F., van Bussel, G. J. and Koutoulakos, E. "Reliability of Different Wind Turbine

Concepts with Relevance to Offshore Application," European Wind Energy Conference & Exhibition, Brussels, Belgium, March 2008.

[13] Windstats (WS), http://www.windstats.com

[14] Landwirtschaftskammer, Schleswig-Holstein, Germany. http://www.lwksh.de/cms

[15] Feng, Y. and Tavner, P. "Introduction to Wind Turbines and their Reliability & Availability", European Wind Energy Conference, Warsaw, Poland, April 2010.

[16] Hameed, Z.; Y.S. Hong, Y.M. Cho, S.H. Ahn, C.K. Song, "Condition monitoring and fault detection of wind turbines and related algorithms: A review," Renewable and Sustainable Energy Reviews, Volume 13, Issue 1, January 2009, Pages 1-39

[17] Wilkinson, M.R.; Tavner, P.J., "Extracting condition monitoring information from a wind turbine drive train," Universities Power Engineering Conference, 2004. UPEC 2004. 39th International , vol.2, no., pp. 591- 594 vol. 1, 6-8 Sept. 2004

[18] Lu, B., Li, Y., Wu, X., and Yang, Z, "A Review of Recent Advances in Wind turbine Condition Monitoring and Fault Diagnosis", IEEE Explore, IEEE Explore, 2009, 978-1-4244-4936.

[19] Lekou, D.J., Mouzakis, F., Anastasopoulo, A.A. and Kourosis, D., "Fused Acoustic Emission and Vibration Techniques for Health Monitoring of Wind Turbine Gearboxes and Bearings", EWEC2009, March 2009.

[20] Christensen, J. and Andersson, C., "Remote Condition Monitoring of Vestas Turbines", EWEC2009, March 2009.

[21] Uluyol, O. Buczak, A. and Nwadiogbu, E. "Neural networks based sensor validation and recovery methodology for advanced aircraft engines," *Proc. SPIE, AeroSense Conference*, Vol. 4389, 102-109, 2001.

[22] Gorinevsky, D., Dittmar, K., Mylaraswamy, D. and Nwadiogbu, E. "Model-based Diagnostics for an Aircraft Auxiliary Power Unit," *IEEE Conference on Control Applications*, 2002. http://www.stanford.edu/~gorin/papers/CCA02diagn.pdf

[23] Mylaraswamy, D. "Addressing the Problem of Early Abnormal Event Detection," *Int. Symp. Proc. Sys. Eng.,*

Fault Diagnosis Conference, pages 240-246, Mumbai, India, 2003.

[24] Kim, K. and Mylaraswamy, D. "Discrete Event Modeling for Fault Diagnosis and Prognosis of Turbine Engines," *ASME TurboExpo, 2006*

[25] Mylaraswamy, D., Olson, L., Nwadiogbu, E. "Engine Performance Trending," *AIAC12-HUMS Conference, 2007*

[26] Bell, Michael B., Foslien, Wendy K., "Early Event Detection-Results From A Prototype Implementation", 2005 Spring National Meeting Atlanta GA, Apr. 10-14, 17th Annual Ethylene Producers' Conference Session TA006-Ethylene Plant Process Control

[27] Stol, K. A. "Geometry and Structural Properties for the CART from Model Tuning," NREL/SR-500-32087, NREL, Golden, CO, September 2004.

[28] Uluyol, O., Kim, K., Ball, C. "Fault Diagnosis and Prognosis for Fuel Supply System in Gas Turbine Engines," *Proceedings of ASME IDETC/CIE, September 24-28, 2005*

[29] Kramer, M. A. "Autoassociative Neural Networks", *Computers and Chemical Engineering.* Vol. 16, No. 4, pp. 313-328, 1992.

[30] Kohonen, T. Self-Organizing Maps, Springer Verlag, Heidelberg, 1995.

[31] Kim, K., Ball, C. and Nwadiogbu, E. "Fault diagnosis in turbine engines using unsupervised neural network technique," SPIE Defense & Security Symposium, Orlando, FL, April 2004.

[32] Johnson, K. E. "Adaptive Torque Control of Variable Speed Wind Turbines," NREL/TP-500-36265, NREL, Golden, CO, August 2004.

[33] Kathryn E. Johnson, Paul A. Fleming, "Development, implementation, and testing of fault detection strategies on the National Wind Technology Center's controls advanced research turbines", Mechatronics, In Press, Corrected Proof, Available online 14 January 2011, ISSN 0957-4158, DOI: 10.1016/j.mechatronics.2010.11.010. (http://www.sciencedirect.com/science/article/B6V43-51Y3WK8-1/2/9a417deb38d5f0c2e37f88654300e0dd)